Available online at www.sciencedirect.com

SCIENCE DIRECT®

Developmental Biology 272 (2004) 328–338

DEVELOPMENTAL BIOLOGY

www.elsevier.com/locate/ydbio

Myosin VI is required for structural integrity of the apical surface of sensory hair cells in zebrafish

Christoph Seiler,[a,1] Orit Ben-David,[b,1] Samuel Sidi,[a] Oliver Hendrich,[a] Alfons Rusch,[c] Beth Burnside,[d] Karen B. Avraham,[b] and Teresa Nicolson[a,*]

[a] *Max-Planck-Institut fur Entwicklungsbiologie, 72076 Tubingen, Germany*
[b] *Department of Human Genetics and Molecular Medicine, Sackler School of Medicine, Tel Aviv University, Tel Aviv 69978, Israel*
[c] *Physiologishes Institut, Eberhard-Karls-Universitat, 72076 Tubingen, Germany*
[d] *Department of Molecular and Cell Biology, University of California, Berkeley, CA 94720, USA*

Received for publication 18 March 2004, revised 30 April 2004, accepted 4 May 2004
Available online 15 June 2004

Abstract

Unconventional myosins have been associated with hearing loss in humans, mice, and zebrafish. Mutations in myosin VI cause both recessive and dominant forms of nonsyndromic deafness in humans and deafness in Snell's waltzer mice associated with abnormal fusion of hair cell stereocilia. Although myosin VI has been implicated in diverse cellular processes such as vesicle trafficking and epithelial morphogenesis, the role of this protein in the sensory hair cells remains unclear. To investigate the function of myosin VI in zebrafish, we cloned and examined the expression pattern of *myosin VI*, which is duplicated in the zebrafish genome. One duplicate, *myo6a*, is expressed in a ubiquitous pattern during early development and at later stages, and is highly expressed in the brain, gut, and kidney. *myo6b*, on the other hand, is predominantly expressed in the sensory epithelium of the ear and lateral line at all developmental stages examined. Both molecules have different splice variants expressed in these tissues. Using a candidate gene approach, we show that *myo6b* is *satellite*, a gene responsible for auditory/vestibular defects in zebrafish larvae. Examination of hair cells in *satellite* mutants revealed that stereociliary bundles are irregular and disorganized. At the ultrastructural level, we observed that the apical surface of *satellite* mutant hair cells abnormally protrudes above the epithelium and the membrane near the base of the stereocilia is raised. At later stages, stereocilia fused together. We conclude that zebrafish *myo6b* is required for maintaining the integrity of the apical surface of hair cells, suggesting a conserved role for myosin VI in regulation of actin-based interactions with the plasma membrane.

Keywords: Myosin VI; Zebrafish; Stereocilia; Hearing; Hair cells; *Satellite*; Snell's waltzer; Gene duplication

Introduction

Vertebrate mechanosensory hair cells in the ear have an apical–basal polarity with a specialized cytoskeleton at the apical surface. Mechanosensitive channels at the tips of apical protrusions transduce small movements triggered by sound or change in body disequilibrium into an electrical signal. The identification of the genes underlying hearing loss in mammals and the functional analysis of the proteins they encode have aided in our understanding of the development and maintenance of hair cells. Much of our knowledge regarding human hearing loss was acquired with animal models, especially the mouse, due to the similarities between the vertebrate inner ear, composed of a cochlea, utricle, saccule, and semicircular canals, and their genomes (Avraham, 2003; Quint and Steel, 2003). Limitations in the mammalian system, however, have led to studies of the zebrafish audiovestibular system, because this vertebrate provides optimal access to the inner ear and hair cells due to ex utero development. Furthermore, the hair cells are visible and can be monitored from early developmental stages (Haddon and Lewis, 1996; Nicolson et al., 1998). Hair cell morphology and physiology, as well as the developmental principles, are similar to that of higher vertebrates (Haddon and Lewis, 1996; Lanford et al., 2000). Most importantly, due to its short generation time

* Corresponding author. Present address: Oregon Hearing Research Center and Vollum Institute, Oregon Health and Science University, 3181 SW Sam Jackson Park Road, Portland, OR 97239. Fax: +1-503-494-2976.
E-mail address: nicolson@ohsu.edu (T. Nicolson).
[1] These authors contributed equally to this work.

0012-1606/$ - see front matter © 2004 Elsevier Inc. All rights reserved.
doi:10.1016/j.ydbio.2004.05.004

and its large number of offspring, zebrafish provide an excellent tool for genetic studies such as large-scale mutagenesis screens and transgene expression.

One of the first genes found to be involved in deafness was the molecular motor myosin VI, initially identified in Snell's waltzer (*sv*) mice (Avraham et al., 1995). Mutations in myosin VI (*MYO6*) underlie nonsyndromic hearing loss (NSHL) DFNA22 and DFNB37 (Ahmed et al., 2003; Melchionda et al., 2001). In *sv/sv* mice lacking myosin VI protein, the stereocilia bundles become disorganized over time and the stereocilia fuse together, resulting in giant stereocilia 20 days after birth (Self et al., 1999). In addition, studies of fibroblasts from *sv/sv* mice showed a reduction in both secretion and the size of the Golgi network (Warner et al., 2003).

The motor protein myosin VI belongs to the family of unconventional or nonclassical myosins and moves toward the pointed (−) end of actin, unlike most other myosins (Wells et al., 1999). Moreover, myosin VI functions as both an anchor and a transporter (Altman et al., 2004). Myosin VI was first identified in *Drosophila* as the 95F myosin heavy chain (Kellerman and Miller, 1992), where it is required for basal protein targeting and spindle orientation in mitotic neuroblasts, as well as epithelial morphogenesis throughout development (Deng et al., 1999; Petritsch et al., 2003). In *Caenorhabditis elegans*, myosin VI is essential for asymmetric segregation of cellular components during spermatogenesis (Kelleher et al., 2000). In mammalian cells, myosin VI is associated with the Golgi complex (Buss et al., 1998) and was suggested to be involved in clathrin-coated vesicle formation, as well as in trafficking of uncoated nascent vesicles (Aschenbrenner et al., 2003; Biemesderfer et al., 2002; Buss et al., 2001). The mammalian myosin VI protein is expressed in a variety of tissues and cells (Avraham et al., 1995; Hasson and Mooseker, 1994); however, in the inner ear, myosin VI is expressed solely in the sensory hair cells (Hasson et al., 1997).

Because of limited accessibility to the sensory organs in mammalian model systems, the zebrafish has acquired a vital role in the auditory and vestibular research areas (Whitfield, 2002). As with other vertebrates, fish sense sound and gravity with the inner ear but they have an additional sensory organ to detect water movements, the lateral line system. The overall organization of the inner ear of zebrafish larvae resembles the mammalian vestibular system, composed of three semicircular canals with one patch of sensory cells in each called crista. In addition, the zebrafish inner ear has two (later three) patches of sensory cells in the macular organ under a stone-like otolith. Like mammalian hair cells, the mechanosensory hair cells of the inner ear and lateral line system have an apical–basal polarity with a hair bundle at the upper surface of the cell. The hair bundle is a collection of highly ordered actin-filled protusions called stereocilia. Deflection of the bundle toward the tallest stereocilia leads to depolarization.

Several large-scale screens for genetic defects have been performed in zebrafish; to date, over 59 mutant loci with inner ear developmental defects have been identified and can be recognized by abnormal ear structure and behavior (Granato et al., 1996; Whitfield et al., 1996). Fourteen mutants were identified with defects specific to inner ear sensory cell function, with many not responding to acoustic vibrational stimuli (Nicolson et al., 1998). These circler mutants have, in addition, a characteristic behavioral phenotype of balance defects.

Despite the pathogenesis caused by myosin VI mutations, the role of this protein in the hair cell is not fully understood. To gain further insight into the cellular basis of deafness associated with myosin VI, we turned to *Danio rerio* (zebrafish). In this study, we present two *myosin VI* genes, designated *myo6a* and *myo6b*, and demonstrate that zebrafish *satellite* (*sai*) mutants harbor mutations in *myo6b*.

Materials and methods

Zebrafish strains

All alleles of *satellite* were generated in the Tübingen (Tü) background. *albino* mutant larvae in Tü background were used for in situ hybridization. All larvae were raised until 120 h postfertilization (hpf) in E3 medium at 30°C. Zebrafish stocks were maintained as described (Haffter et al., 1996).

Mapping of myo6a and myo6b

We used the zebrafish Goodfellow T51 radiation hybrid panel to physically map *myo6a* and *myo6b*. Amplification was performed as previously described (Geisbrecht and Montell, 2002). The mapping prediction on the T51 panel map was performed using the "It's *Cool!* and It's *Hot!* Instant Mapping" website from The Children's Hospital Zebrafish Genome Project Initiatives http://www.zfrhmaps.tch.harvard.edu/ZonRHmapper/instantMapping.htm).

The PCR band patterns derived from the genomic DNA of each radiation hybrid cell line for *myo6a* was (1: PCR band, 0: no band, 2: uncertain): 001000001100000-000000000000001000000000000000010000100000000-000110011001100000001010000000000101. The mapping patterns for *myo6b* was 001000001000100000000010010-010000000000000000000000000200100000000000000001-000000101000000000001.

Cloning of myo6a and myo6b

The bass myosin VI (Breckler et al., 2000) was used to identify zebrafish myosin gene *myo6a.* Primers designed from a portion of the globular domain of the tail from the bass myosin VI isoform FMVIA (3642f-5′ GGATATGTGT-GAGCTGAGTCTGGAG 3′ and 3807r-5′ CATGGCTGTG-GCGTAGGTGG 3′) were used to amplify zebrafish genomic DNA. The ^{32}P-dCTP labeled product was used to screen an adult zebrafish kidney cDNA library. Hybridization was done with Church buffer at 65°C. Posthybridization washes were done in 0.1× SSC, 0.1% SDS, 40 mM sodium phosphate pH

7.2 at 65 °C. Clones were then obtained from RZPD (German Resource Center for Genome Research, Berlin) according to the coordinates that were found. Approximately 70% of the gene, including the 3′ UTR, was obtained from these clones. The 5′ end could be predicted from both ESTs and the genomic contigs. The sequence was confirmed by sequencing PCR products obtained using primers generated from the predicted sequence on cDNA from 5-day-old larvae.

To search for additional *myosin VI* genes, a fragment from the tail domain of mouse *myosin VI* corresponding to amino acids 1012–1264 (Genbank Accession No. NM_008662) was used to search the draft sequence of the zebrafish genome using Ensembl BLAST (http://www.ensembl.org/Danio_rerio/blastview). This revealed one contig containing sequences from *myo6a* and another one similar but not identical to the first. We confirmed that the new gene, designated *myo6b*, is a *myosin VI* paralogue by performing BLAST analysis against the identified contig and found that a large portion of the coding sequence was identical to human *MYO6*, with less identity to other myosins. Approximately 80% of the gene, including the 5′ end, could be predicted from the genomic contigs. The sequence was then confirmed by sequencing PCR products obtained using primers generated from the predicted sequence on cDNA of adult zebrafish. The 3′ end was amplified by RACE PCR using the Marathon RACE Kit (Clontech) with cDNA from 5-day-old larvae. The 5′ end was confirmed by RACE using the same method.

Mapping and sequencing of satellite

For genetic mapping of *satellite*, the allele *tn3137* was used. The mutation was generated in the Tü background; for mapping, carriers were crossed with wild type from the background wik. Linkage analysis was performed using PCR-able (CA)n SSLP markers as described previously (Knapik et al., 1998; Talbot and Schier, 1999).

For sequencing of the *satellite* alleles, total RNA was isolated from 3- to 5-day-old larvae using the Nukleospin RNAII kit (Macherey Nagel). cDNA was amplified using the Advantage RT for PCR Kit (Clontech). For sequencing, three overlapping fragments of *myo6b* were amplified, precipitated using EtOH and sodium acetate and used directly for sequencing.

In situ hybridization

Whole-mount in situ hybridization was performed as described previously (Hammerschmidt et al., 1996; Schulte-Merker et al., 1994). The coding sequence from *myo6a* corresponding to 3175–3630 bp was used as a probe. The coding sequence corresponding to 3023–3522 bp was used for *myo6b* expression.

Fluorescent staining and microscopy

Fluorescent labeling of lateral line neuromasts with FM1–43 (Molecular Probes) was performed as previously described (Seiler and Nicolson, 1999). Day 5 larvae were stained for 30 s in E3. For phalloidin staining of hair bundles, 5-day-old larvae were fixed overnight in 2% glutaraldehyde/1% paraformaldehyde in Ringer solution (145 mM NaCl, 3 mM KCl, 1.8 mM $CaCl_2$, 10 mM HEPES pH 7.2). The larvae were then treated for 24 h with 2% Triton-X100 at 4 °C in the presence of fixative, washed four times and stained for 24 h (4 °C) with 10 U/ml Alexa488-Phalloidin (Molecular Probes). For confocal microscopy, an inverted Leica DM IRBE microscope equipped with a 100× oil lens was used. For live images (FM1-43), 5-day-old larvae were anesthetized with MESAB (0.02% 3-amino-benzoic acid ethyl ester) and examined under an Axiophot microscope equipped with a Zeiss Axiocam. The settings including the exposure time were optimized with wild-type larvae and not changed for the mutant larvae.

Light microscopic images of live fish were taken with a 60× water immersion lens and a CoolSnap digital camera (Roper Scientific, Tuscon, AZ) using Metamorph software (Universal Imaging Corp., Downingtown, PA).

Electron microscopy

For electron microscopy, larvae were processed as previously described (Seiler and Nicolson, 1999). Briefly, larvae were fixed in 2% glutaraldehyde/1% paraformaldehyde in Ringer solution. Whole larvae were embedded in Epon and oriented in a way such that the ear was sectioned in a transverse dorsal to ventral direction. To characterize and compare the phenotype of *sai* in different alleles and different stages, we examined 4 and 8 dpf larvae of the alleles *tn011* and *jq392* (each $n = 1$), 5 dpf larvae of the allele *tn3216* ($n = 1$), and 4 dpf ($n = 2$), 5 dpf ($n = 3$), and 8 dpf ($n = 2$) larvae of the allele *tn3137*.

Microphonic potentials of hair cells

Extracellular receptor potentials were recorded as previously described (Nicolson et al., 1998).

Results

Identification of two myo6 loci in zebrafish

To establish a zebrafish model for myosin VI-associated deafness and to obtain insight into the function of the gene in the inner ear, we searched for zebrafish myosin VI and subsequently identified two genes, designated *myo6a* and *myo6b*, both homologues of the human *MYO6*. *myo6a* was detected by amplification from zebrafish genomic DNA with primers made from the globular domain of the bass myosin VI isoform FMVIA (Breckler et al., 2000). The product was used to screen an adult zebrafish kidney cDNA library. Using the zebrafish T51 radiation hybrid panel, *myo6a* mapped on LG 20 near to the EST fc83h02 (Fig. 1A). A portion of *myo6b*

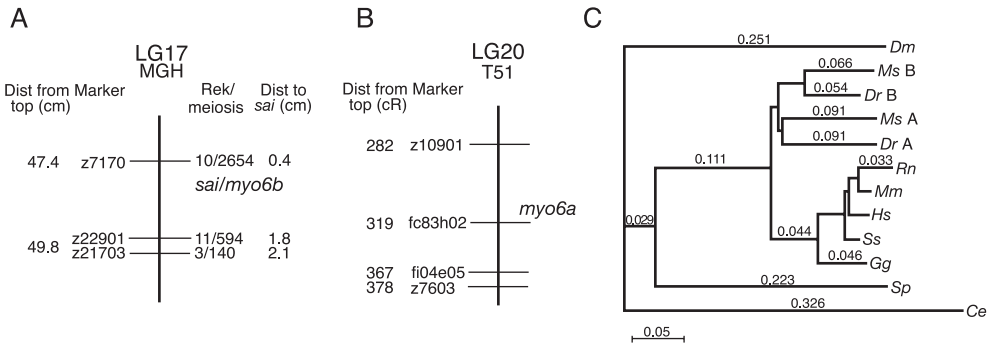

Fig. 1. *myosin VI* is duplicated in zebrafish. (A, B) Mapping of *myo6a* and *myo6b*. (A) *myo6a* maps to chromosome 20 between the markers fi04e05 and z10901. (B) *satellite* (*sai*) was mapped to chromosome (LG) 17 between the markers z7170 (10 recombination events/2654 meiosis) and z22901 (11 recombinations/594 meioses). *myo6b* mapped to the T51 radiation hybrid map in the same area. (C) Phylogenetic relationship of myosin VI proteins. Unrooted phylogenetic tree was constructed in MacVector7 (accelrys) using clustalW alignment. Full-length amino acid sequences of the proteins were used. *Danio rerio Dr A*; *Danio rerio Dr B*. Accession numbers of the proteins used for the phylogenetic tree are NP_032688 (*Mus musculus*, *Mm* myosin VI), AAC51654 (*Homo sapiens*, *Hs* myosin VI), AAA97927 (Caenorhabditis elegans, *Ce* hum-3), A54818 (*Sus scrofa domestica*, *Ss* myosin VI), AAD52005 (*Morone saxatilis*, *Ms* A FMVIA), AAD52006 (*Morone saxatilis*, *Ms* B FMVIB), Q01989 (Drosophila melanogaster, *Dm* 95F MHC-Jaguar protein), XP_236444 (*Rattus norvegicus*, *Rn* Myosin VI), CAB96536 (*Gallus gallus*, *Gg* myosin VI), AAF72178 (*Strongylocentrotus purpuratus*, *Sp* myosin VI). The scale indicates phylogenetic distance by substitution events.

was identified by BLAST analysis with the mouse sequence against the draft sequence of the zebrafish genome and used to determine its chromosomal location. *myo6b* mapped on LG 17 in proximity to the z-Marker z7170, in the region where the *satellite* locus was mapped (Fig. 1B).

Isolation and characterization of myo6a and myo6b

Approximately 70% of *myo6a* was obtained by screening an adult zebrafish kidney cDNA library including the 3′ UTR. The 5′ end of the gene was predicted from genomic sequence and EST clones and was confirmed by RT-PCR. Approximately 80% of *myo6b*, including the 5′ end, was predicted from genomic sequence and was confirmed by RT-PCR and by RACE-PCR with cDNA from 5-day-old larvae. The 3′ end of the *myo6b* was obtained by RACE-PCR with cDNA from 5-day-old larvae.

As in all myosins, the zebrafish myosin VI proteins consist of a head, a neck and a tail region, and the domain structure of these regions is conserved with the other known myosin VI molecules. The head or motor domain contains an ATP-binding site and an actin-binding domain. This catalytic domain is followed by a head insertion of approximately 53 amino acids, which is unique to myosin VI, and an IQ motif, both of which are thought to compose a lever arm that confers directionality of myosin VI movement (Fig. 2) (Wells et al.,

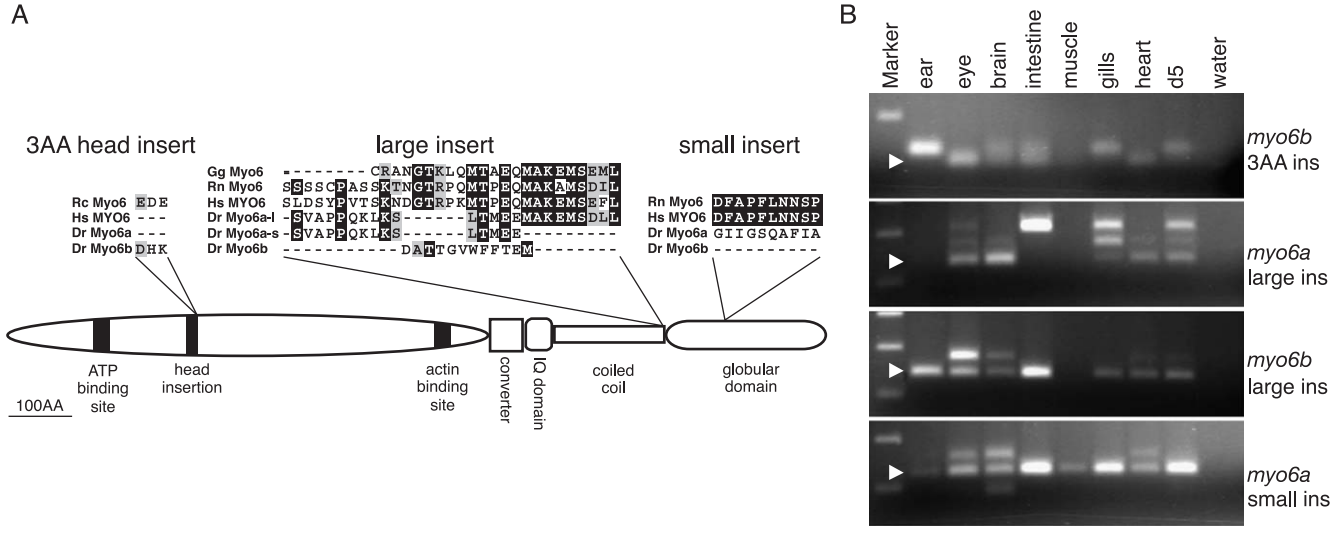

Fig. 2. Splice variants of *myo6a* and *myo6b* and their expression in adult zebrafish tissues. (A) Two sites with differential splicing within the tail domain are present in *myo6a*. The large insert between the coiled coil domain and the globular domain has two different sizes (Dr Myo6a-l and Dr Myo6a-s). A small insert is present within the globular domain. In *myo6b* mRNA, the large insert within the tail domain is also present and there is an additional site after the head insertion. (B) Expression of the various splice forms in different adult tissues (arrowhead indicates the forms without insert). Gg: *Gallus gallus*; Rn: *Ratttus norvegicus*; Hs: *Homo sapiens*; Dr: *Danio rerio*; Rc: *Rana catesbeiana*.

1999). The tail consists of a coiled coil domain and a globular domain (Fig. 2). Myo6a has a predicted length of 1292 amino acids (AA) and Myo6b has a predicted length of 1267 AA. The proteins share high AA homology of 82% (76% on the nucleotide level). The head and neck regions have a slightly higher conservation (both 87%) than the tail region (78%).

Phylogenetic tree of Myo6 proteins

To address the phylogenetic relationship among the *myosin VI* genes, an unrooted phylogenetic tree based on the predicted amino acid sequence was constructed using the Clustal W program (Fig. 1C). When constructing a phylogenetic tree based only on the predicted head domain, the evolutionary distance decreases, further indicating that the head is the most conserved domain.

When comparing the entire lengths of the proteins, the fish homologues are on one branch, while the mammalian genes are on a different branch, very close to the *Gallus gallus* (chicken) myosin VI. Myo6 was found to be duplicated in another distantly related fish, the striped bass (*Morone saxatilis*) (Breckler et al., 2000). Although *M. saxatilis* and *D. rerio* are from distantly related orders [Perciformes (perch-likes) and Cyprinoformes (carps), respectively] the Myo6a proteins from bass and zebrafish are in one branch and the Myo6b proteins in another. This may be explained by a genome duplication event in fish that occurred after the divergence of ray-finned fishes and lobe-finned fishes, from which the mammalian lineage evolved (Prince and Pickett, 2002; Taylor et al., 2003). Our study suggests that this duplication happened before the split of the perch and carp lineage.

Alternative splice forms of myo6a and myo6b

Two different sites of alternative splicing have been described in the tail domain of myosin VI. These include one large insert between the coiled coil region and the globular domain (Breckler et al., 2000; Buss et al., 2001), and a small insert within the globular domain.

The large insert has been shown to be required for clathrin-dependent endocytosis and is expressed in polarized cells (Buss et al., 2001). In zebrafish, we detected this insert in both *myo6a* and *myo6b*. The length of the large insert varies in different species; in human, it consists of 20 amino acids, while in the bass, Myo6a has 13 amino acids (Breckler et al., 2000; Buss et al., 2001). In zebrafish Myo6a, there are two variants of the large insert, a variant with 24 amino acids and a variant that contains only the first 11 amino acids. In Myo6b, there is one splice variant of 12 amino acids (Figs. 2A,B). The 24 amino acid variant of Myo6a has high amino acid similarity to the large insert of *Rattus norvegicus* (rat), *Mus musculus* (mouse), *Homo sapiens* (human), and *G. gallus* (chicken). The 11 amino acid variant of *myo6a* and the *myo6b* large insert from zebrafish, as well as the large insert described for *myo6*a and *myo6b* in the bass (Breckler et al., 2000), have no similarity to mammalian and chicken myosin VI.

These inserts are too small to be detectable by whole-mount in situ hybridization. To investigate their expression, we prepared cDNA of different adult tissues (Fig. 2B). The 24 amino acid form of the Myo6a large insert is expressed in intestine and gills; the 11 amino acid variant is detectable in the gills. The large insert of Myo6b could only be detected in the eye and brain, while the form with no insert is present mainly in cDNA from the eye, ear, and intestine.

The small insert splice variant could only be detected in zebrafish *myo6a*, as an insert of 10 amino acids but not in zebrafish *myo6b*. The small insert is fully conserved between the mammals but not in zebrafish or striped bass. The small tail insert of *myo6a* is expressed in the eye and brain with very weak expression in the heart.

Using RT-PCR analysis on 5-day-old larvae, we detected an additional three amino acids insert immediately after the head insertion in about 40% of the *myo6b* transcripts. These amino acids leads to the addition of a putative casein kinase II (CK2) phosphorylation site [consensus S/T-(X)2-D/E, here SPED]. In adult tissues, these additional amino acids were detected mainly in the ear but not in the eye (Fig. 2B, top panel). Very weak expression was also detectable in the gills, intestine, and brain.

We performed a BLAST protein database search to identify other myosin VI orthologues with similar insertions. We found a fragment from *Rana catesbeiana* (bullfrog), which also contained three additional amino acids after the head insertion (Accession No. AAA65090 and AAA65079). A putative caseine kinase phosphorylation site is present due to this domain as well (here SPEE instead of SPED), increasing the likelihood that this quite short domain is indeed functional.

myo6a and myo6b are expressed in different organs

To determine the spatial and temporal expression of *myo6a* and *myo6b*, we performed in situ hybridization with 1, 3, and 5-day-old whole larvae. In 1-day-old larvae, *myo6a* is expressed in the anterior neuroectoderm and the trunk, with strong expression in the pronephros (Figs. 3A,B). In 3-day-old (data not shown) and 5-day-old larvae, *myo6a* is expressed in the brain, the gills, the mesonephros (kidney) and in the gut (Figs. 3C, D). The weak expression in the swim bladder and inner ear is most likely nonspecific and due to collection of dye in these closed cavities. This expression was also present when stained with the sense probe, while the other signals were specific for the antisense probe (data not shown).

myo6b is specifically expressed in the sensory hair cells (Figs. 3E–H), which is consistent with our finding that mutations in this gene lead to the *satellite* mutant phenotype. At day 1, *myo6b* is expressed in the precursors of the sensory hair cells, the tether cells, at the anterior and posterior part of

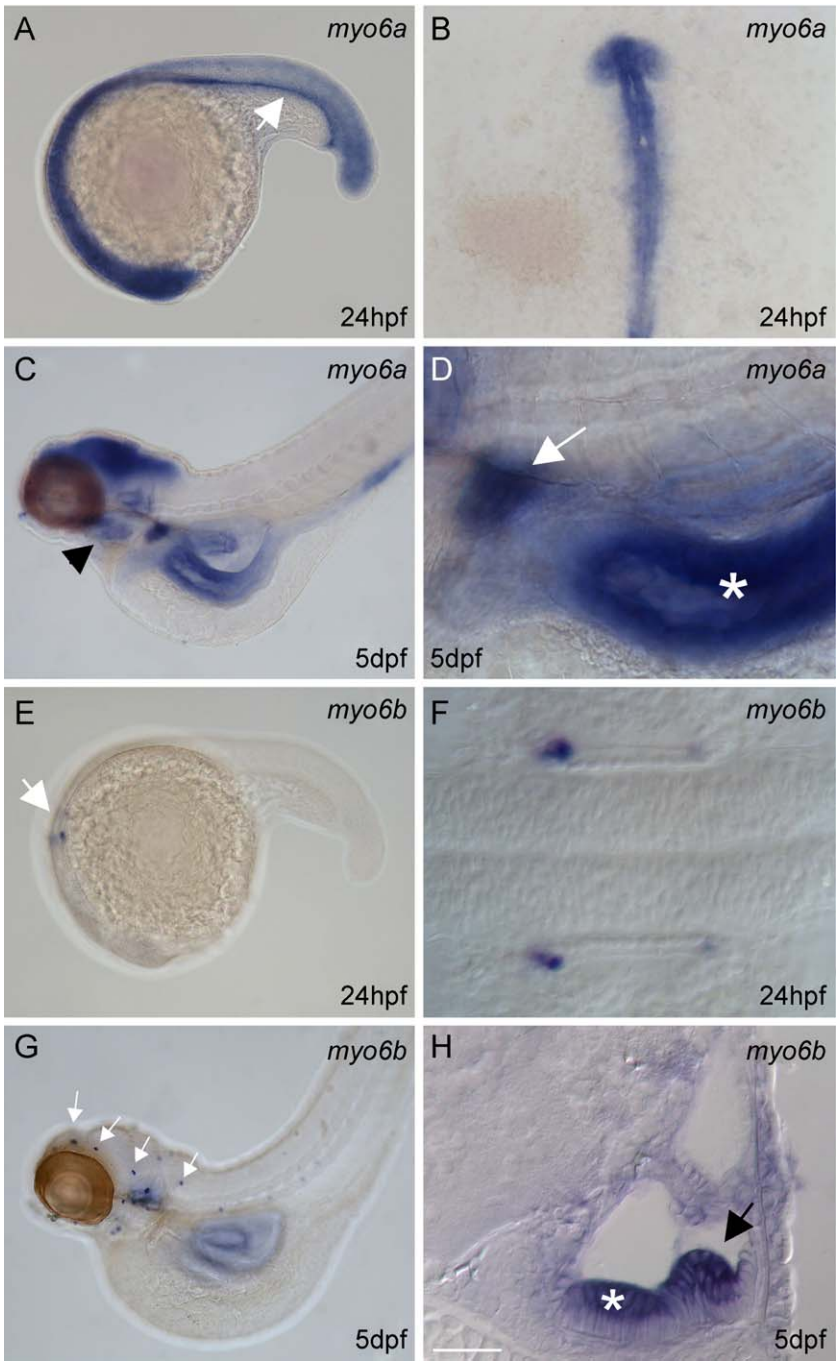

Fig. 3. Expression patterns of *myo6a* and *myo6b* in the developing zebrafish. At 24 hpf, *myo6a* is expressed throughout the whole embryo with strong expression in the anterior neuroectoderm (B) and the pronephric duct (A; arrow). At 5 dpf, *myo6a* is expressed in the mesonephros (kidney) (arrow in D), intestine (C, D; asterisk in D) and brain. (C) Weak expression is visible in gills (C, arrowhead). *myo6b* is expressed in mechanosensory hair cells; at 24 hpf (E, F) in the first hair cells of the otic placode (arrow in E), and at 5 dpf in the inner ear and neuromasts (G; neuromasts indicated with arrows). (H) A cryosection of a larval ear stained as in G, showing expression of *myo6b* in hair cells of the utricular macula (asterisk) and lateral crista (arrow). Scale bar in H indicates 50 μm in A, B, D, E, 225 μm in C, G, and 25 μm in F, H.

the otic vesicle (Figs. 3E, F). At day 3 (data not shown) and day 5, *myo6b* is expressed in the patches of sensory hair cells of the inner ear and lateral line organ (Figs. 3G, H). After prolonged staining, expression was also detectable in the intestine at 5 dpf (not shown). No staining was seen in these areas with the sense probe (data not shown).

Identification of myo6b as satellite

The zebrafish *myo6b* maps near the *satellite* (*sai*) locus (Fig. 1B). *satellite* is one of a total 24 loci related to a deafness phenotype that have been identified in recent screens (Granato et al., 1996; Nicolson et al., 1998; T. Nicolson,

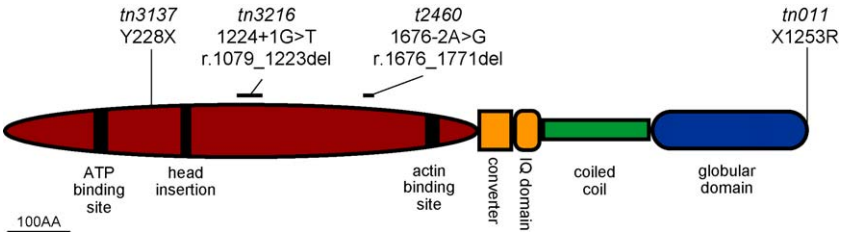

Fig. 4. Diagrammatic representation of zebrafish myosin VI and the mutations in *satellite/myo6b*. Myosin VI is comprised of three parts—head (red), neck (orange), and tail (green and blue)—containing several domains as indicated in the figure. Sequencing of *myo6b* from *sai* mutant larvae revealed mutations in four alleles. *tn3137* causes a truncation of the protein (Y228X). *tn3216* leads to a deletion of a 145-bp exon (r.1079_1223del) caused by a mutation in the splice donor site (1224 + 1G > T) resulting in a frameshift. *t2460* has a in frame deletion of a 96-bp exon (r.1676_1771del) due to a mutation in the acceptor site (1676-2A > G). *tn011* has a mutation removing the stop codon (X1253R).

unpublished results). Mutations in *satellite* cause one of the weaker phenotypes of this class, because all mutants carrying one of the five alleles. However, all *satellite* mutants have an obvious vestibular defect resulting in uncoordinated swimming.

Sequencing of *myo6b* from mutant larval cDNA or genomic DNA revealed four different mutations in four alleles of *satellite* (Fig. 4). We were unable to detect a mutation in the open reading frame of the fifth allele. In the allele sai^{tn3137}, we found a nonsense mutation at codon 228, 684T → A, leading to a premature stop codon (Y228X) (Fig. 4). The presumed truncation occurs in the head of Myo6b, distal to the ATP binding domain. The allele sai^{tn011} has a nonsense mutation at the stop codon, 3802T → C, leading to removal of the generic stop codon (X1268R) (Fig. 4). Because no alternative stop codon is present in the UTR, the mutation adds 29 amino acid residues that are followed by the polyA tail at the nucleotide level. In the allele sai^{t2460}, we found a mutation in the splice receptor, 1684(−2)A → G, leading to an in-frame deletion of a 96-bp exon (Fig. 4). The allele *tn3216* harbored a mutation in the splice donor, 1078(+ 1)G → T, leading to a deletion of 145-bp exon, ending with a frameshift and a premature stop codon (Fig. 4).

Functional analysis of satellite hair cells

To determine if the function of mutant *satellite* hair cells was compromised, we measured the microphonic potentials of hair cells of the lateral line system. This noninvasive method measures the extracellular receptor potentials of hair cells upon mechanical stimulation (Nicolson et al., 1998). In wild-type larvae, the average measured extracellular receptor potential of the hair cells of one neuromast was 17.3 μV. The extracellular receptor potentials in the presumed null allele sai^{tn3216} were reduced by about 83% (to 2.98 μV) (Fig. 5A). Zebrafish circler mutants or *nompC* morphants that have reduced or absent extracellular receptor potentials, also have reduced labeling or do not take up the styryl dye FM1–43 (Ernest et al., 2000; Seiler and Nicolson, 1999). To investigate if *satellite* mutants have reduced or normal uptake of FM1–43 in lateral line hair cells, we compared mutant *satellite* larvae to wild-type larvae (Figs. 5B–D). Although the uptake of FM1–43 was strongly reduced, some staining was still visible in mutant hair cells (Figs. 5B–D; Table 1). These results were consistent with the reduction in extracellular receptor potentials.

A

	Mean (μV)	S.D.	n of Larvae	n of Neurom.
WT	17.3	4.9	5	10
tn3216	2.98	0.6	3	5

Fig. 5. Extracellular receptor potentials and FM1–43 uptake are reduced in mutant *satellite/myo6b* hair cells (5 dpf). (A) Electrical responses in hair cells to mechanical stimuli are reduced in larvae carrying the *tn3216* allele. Comparison of FM1–43 labeling in wild type (B), *tn3137* (C), and *tn011* (D) larvae shows a marked reduction of uptake in mutant *satellite* hair cells. Scale bar, 50 μm.

Table 1
Summary of defects in mutant satellite/myo6b larvae

Allele	Acoustic startle reflex[a]	Apical surface	Microphonics (μV)	FM1–43 uptake[b]
Wild type	+	Normal	17.3	+
tn3137	+/–	Abnormal	n.d.	+/–
tn3216	+/–	Abnormal	2.98	+/–
t2460	+/–	Abnormal	n.d.	+/–
tn011	+/–	Abnormal	n.d.	+/–

[a] + indicates normal responses to stimuli (tapping on petri dish); +/– indicates that some larvae do not respond to every stimulus.
[b] + indicates normal uptake; +/– indicates severely reduced uptake.

Fine structure analysis of mutant satellite hair bundles

The phenotype of fused stereocilia is striking in *sv* mutant hair cells (Self et al., 1999). Using light microscopy, we could discern hair bundle defects in live, undissected mutant larvae (Fig. 6). Many bundles did not have a stereotypical conical shape as seen in wild-type larvae (Figs. 6A,C), and appeared to be malformed, shorter, or thinner (Figs. 6B,D). To examine the structural integrity of hair bundles in *satellite* mutants in more detail, we labeled the actin filaments in hair bundles of the inner ear in intact larvae using fluorescent phalloidin. Labeling with Alexa488-phalloidin revealed a variable and moderate degree of disorganization of the ampullary hair bundles in *satellite* mutants, with occasional splitting of stereocilia (Figs. 7A–D). As in the live images, the bundles often appeared shorter and in some cases, thinner than wild-type bundles. To further analyze the morphology of mutant hair cells, we examined ultrathin sections of the inner ear macula organ using transmission electron microscopy (TEM) (Figs. 7E–H). In *satellite* mutant maculae, the morphological defects varied (see Table 2). In some hair cells, the cuticular plate, a dense actin meshwork under the stereociliary bundle, was present but was often bulging out above the epithelium (Fig. 7G). In addition, the spread of the apical surface appeared narrower than in wild-type bundles. Most mutant hair cells had vesicles not only at the pericuticular necklace, which is situated between the cuticular plate and the lateral membrane, but also within the cuticular plate itself (Figs. 7F, G). As seen in Fig. 7H, the membrane at the apical surface appeared to climb up the bases of the stereocilia and the stereocilia appeared thicker in several hair cells. We examined animals at different stages (4, 5, and 8 dpf) and observed a progressive increase in the number of hair cells with a more severe phenotype as depicted in Figs. 7G and H (Table 2).

Discussion

Myosin VI has been intensively studied in the last years in an attempt to reveal its biological function and to understand its role in the process of hearing. Knowledge has been acquired regarding the myosin VI backward movement along actin filaments (Homma et al., 2001; Nishikawa et al., 2002; Wells et al., 1999) and the role of myosin VI in vesicle movement and vesicle formation (reviewed in Hasson, 2003), but the function of myosin VI in hair cells has not been fully explored. We propose *satellite* as a zebrafish model for human myosin VI-associated deafness, with zebrafish Myo6b serving as an aid in further understanding the role of myosin VI in the hair cells.

Exclusive expression patterns of the myo6 gene duplicates

We show that in zebrafish, there are two different genes corresponding to the mammalian myosin VI gene, with differing expression patterns. The combined expression patterns of the two zebrafish paralogues resemble the expression pattern of mammalian myosin VI. In mice, *Myo6* is ubiquitously expressed with high levels in the brain, kidney, and lung (Avraham et al., 1995). The expression of myosin VI in the murine inner ear is restricted to the hair cells (Hasson et al., 1997). In the zebrafish, *myo6a* is highly expressed in the brain, kidney, and gut, whereas *myo6b* expression is restricted to the hair cells and the adult eye.

Two alternative splice sites have been described for myosin VI in vertebrates; the expression of the splice variants varies in different tissues (Breckler et al., 2000; Buss et al., 2001). In zebrafish, we also detected these alternative splice sites and observe tissue-specific expression of various *myo6* splice variants. A large insert between the coiled coil and the globular domain that has been shown to be involved in targeting of myosin VI to clathrin-coated vesicles, exists in both zebrafish *myo6a* and *myo6b*. The

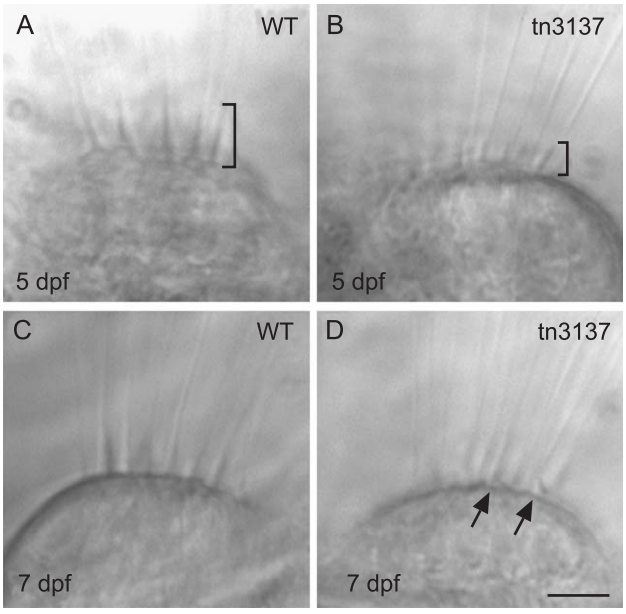

Fig. 6. Hair bundles are abnormal in live mutant *satellite* fish. Shown are hair cells from the medial cristae of the inner ear. (A, C) Wild-type hair bundles in 5 and 7 dpf larvae. (B, D) Mutant *satellite* hair bundles at the same stages. The brackets indicate the length of the tallest stereocilia. Arrows point to abnormalities near the surface of the neuroepithelium. Scale bar, 3 μm.

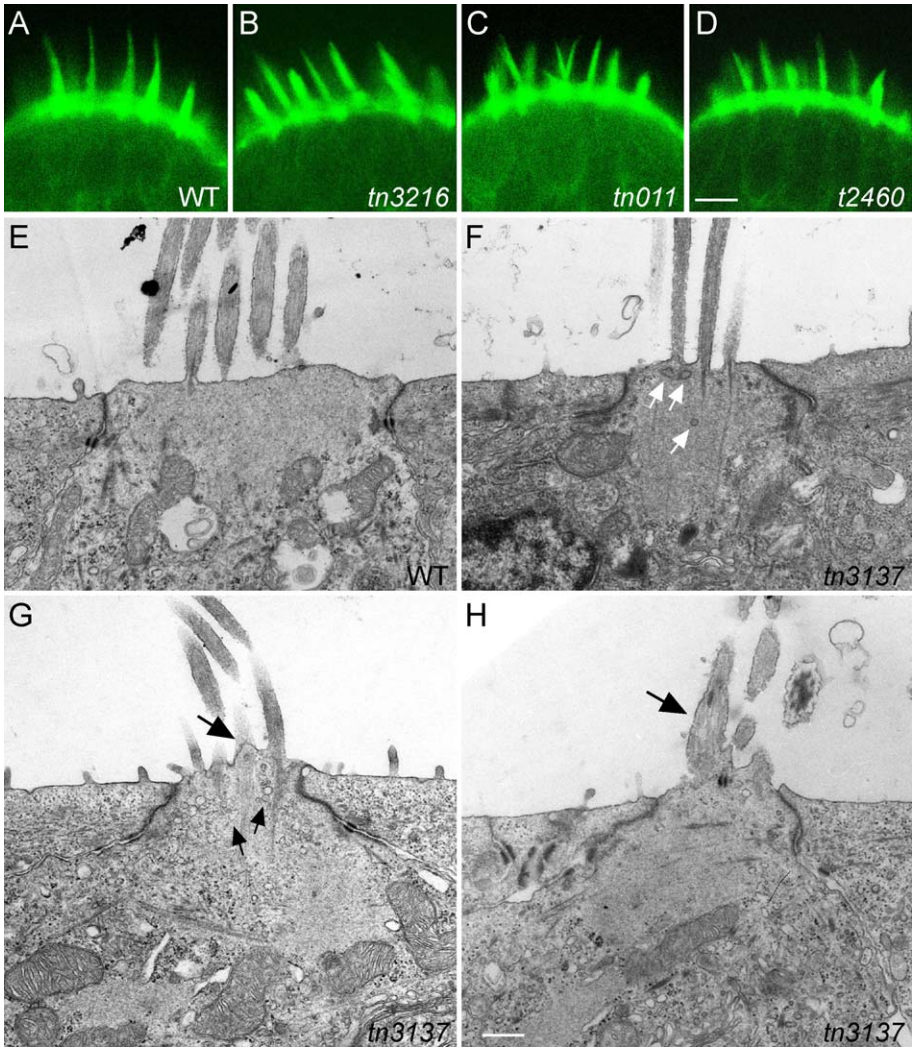

Fig. 7. Defects in the structural integrity of the apical surface in mutant *satellite/myo6b* hair cells. (A–D) Confocal images of ampullary hair bundles of the inner ear labeled with Alexa488-phalloidin (6 dpf). Split bundles are detectable in *tn3216* (B) and *t2460* (C) larvae. (E–H) Transmission electron micrographs of hair bundles in wild-type (E) or *tn3137* (F–H) anterior (utricular) maculae (5 dpf). Defects ranged from mild accumulation of vesicles (F, white arrows; G, small arrows) to raised membrane (G, large arrow) and fusion of stereocilia (H, large arrow). Scale bar in D indicates 2 μm in A–D; and scale bar in H indicates 500 nm in E–H.

large insert present in *myo6a* shows homology to the corresponding splice form identified in other vertebrates. This particular splice variant of *myo6a* is highly expressed in the intestine, which is consistent with a role in clathrin-mediated endocytosis in this tissue. In contrast, we do not detect expression of the large insert variant of *myo6b* in the ear. We also report additional splice variants that may affect the function of the globular domain and the head domain. Further studies may elucidate the impact of these additional amino acid insertions on myosin VI function.

Table 2
Progression of morphological defects in *satellite*^{tn3137} hair cells examined

	4 dpf	5 dpf	8 dpf
Number of hair cells			
Wild type	12	11	14
tn3137	17	23	16
Normal apical surface			
Wild type	100%	100%	100%
tn3137	70%	73%	37%
Elevated apical membrane			
Wild type	0%	0%	0%
tn3137	30%	27%	44%
Fused stereocilia			
Wild type	0%	0%	0%
tn3137	0%	0%	19%

Gene duplication events are common phenomena during evolution, especially among fish, in which a large-scale gene duplication event occurred (Taylor et al., 2003). In most cases, one of the duplicated pairs degenerates while the other retains its original function; in other rare cases, the duplicated pair gains a new function. According to the duplication–degeneration–complementation model (Force et al., 1999; Prince and Pickett, 2002), duplicated genes can also "split function" after the duplication event such that both genes are required to complement full function of the ancestral gene. These events can explain the different roles

of closely related genes in various tissues or during different developmental stages. The two homologous *myo6* genes are highly similar and conserved among other vertebrates, indicating that the function of the protein is conserved. Thus, the different expression patterns suggest that the *myo6* duplicated pair are functionally complementary, and as such, provide a powerful tool for further understanding the specialized role of *myo6* in the inner ear.

Role of myo6b in zebrafish hair cells

The chromosomal location of *myo6b* made it an attractive candidate for the circler gene, *satellite* (*sai*). Indeed, we found *myo6b* mutations in four alleles of *satellite*. The mutations in the sai^{tn3216} and sai^{tn3137} alleles presumably give rise to truncated proteins containing only part of the head domain and hence, are probably null mutations. In the sai^{t2460} mutant, there is a loss of an exon in the head domain, most likely affecting the head structure and/or function. In the sai^{tn0111} allele, there is an addition of more than 29 amino acid residues at the carboxy terminal end of the protein that may affect protein stability and the function of the tail domain.

Extracellular receptor potentials or uptake of FM1–43 is severely reduced in *satellite* mutant hair cells, suggesting that mechanotransduction is compromised. Our data suggests, however, that *myo6b* is not directly involved in the transduction complex, but rather, is required for structural integrity of the mechanosensory cells. Phenotypic analysis of hair-cell morphology in *satellite* mutants revealed structural defects at the apical surface. The hair bundles were irregular in appearance and in some cases, split apart. Although not a fully penetrant phenotype, the cuticular plate often protruded above the epithelium with the apical plasma membrane rising along the bases of the stereocilia. We found that the phenotype in *satellite* mutant hair cells is progressive, becoming more severe at later stages. Disorganized bundles and raised membrane were also observed in the hair cells of Snell's waltzer mice 3–7 days after birth (Self et al., 1999). An additional phenotype seen in *satellite* mutant hair cells was the accumulation of large vesicles near or within the cuticular plate. A number of studies have implicated myosin VI in vesicle formation or trafficking (Buss et al., 2002; Hasson, 2003). Uptake of FM1–43, which is reduced in mutant *satellite* hair cells, appears to occur via endocytosis in zebrafish hair cells in a mechanotransduction-dependent manner (Seiler and Nicolson, 1999). The accumulation of vesicles and reduction of endocytosis suggests a possible defect in vesicle trafficking. Recently, Aschenbrenner et al. (2004) have shown that Myo6 is required for the transport of uncoated vesicles through actin dense areas in polarized cells. The isoform used in their study does not contain the large tail insert (Hasson and Mooseker, 1994), and is thus homologous to the isoform we detected in zebrafish ears. We only rarely detected vesicles within the cuticular plate in wild-type larvae, suggesting that the absence of *myo6b* function results in an accumulation of vesicles within the cuticular plate. Moreover, myosin VI is concentrated within the vesicle-rich pericuticular zone surrounding the cuticular plate in hair cells (Hasson et al., 1997), suggesting a role in endocytosis or trafficking within this specialized region of hair cells. However, it is not clear if the accumulation of vesicles is a secondary defect as such a phenotype is present in zebrafish hair cells undergoing degeneration (T. Nicolson, unpublished observations). An accumulation of vesicles in hair cells was not noted in Snell's waltzer mice and endocytosis did occur in mutant hair cells, although it was not measured quantitatively (Self et al., 1999). Raised membrane, on the other hand, is present in both *sv*/*sv* mice and *satellite* zebrafish mutants. This common defect suggests that myosin VI plays an important role in tethering the apical membrane to the cuticular plate. Consistent with this notion, myosin VI is highly abundant within the cuticular plate (Hasson et al., 1997). It is also concentrated in other polarized epithelial cells within a similar actin meshwork, the terminal web (Hasson and Mooseker, 1994). It has been postulated that the dimerization of the coiled-coil domain of myosin VI may allow it to play a structural role within such meshworks with the C-terminal globular domain providing an anchor to the membrane-bound proteins (Hasson and Mooseker, 1996). A recent study suggests that myosin VI is able to switch from being a translocator to an anchor molecule, depending on the load applied to the motor (Altman et al., 2004). The defects observed in *satellite* mutants are consistent with a model of myosin VI serving as an anchor protein critical for stabilizing and regulating membrane interactions with actin filaments.

Our study establishes the *satellite* mutant as an alternative animal model for human hereditary deafness associated with myosin VI. Based on the phenotype described here, we suggest that myosin VI plays an evolutionarily conserved role in maintaining the integrity of the apical surface of hair cells.

Acknowledgments

We thank Hashem Shahin. This work was supported by the Israel Ministry of Health (KBA), NIH R01 DC005641 (KBA) and SFB 430 and DFG funding (TN). This work was performed in the partial fulfillment of the requirements for a PhD degree of Orit Ben-David, Faculty of Medicine, Tel Aviv University, Israel.

References

Ahmed, Z.M., Morell, R.J., Riazuddin, S., Gropman, A., Shaukat, S., Ahmad, M.M., Mohiddin, S.A., Fananapazir, L., Caruso, R.C., Husnain, T., Khan, S.N., Riazuddin, S., Griffith, A.J., Friedman, T.B., Wilcox, E.R., 2003. Mutations of MYO6 are associated with recessive deafness, DFNB37. Am. J. Hum. Genet. 72, 1315–1322.

Altman, D., Sweeney, H.L., Spudich, J.A., 2004. The mechanism of myosin VI translocation and its load-induced anchoring. Cell 116, 737–749.

Aschenbrenner, L., Lee, T., Hasson, T., 2003. Myo6 facilitates the translo-

cation of endocytic vesicles from cell peripheries. Mol. Biol. Cell 14, 2728–2743.

Aschenbrenner, L., Naccache, S.N., Hasson, T., 2004. Uncoated endocytic vesicles require the unconventional myosin, myo6, for rapid transport through actin barriers. Mol. Biol. Cell. 15, 2253–2263.

Avraham, K.B., 2003. Mouse models for deafness: lessons for the human inner ear and hearing loss. Ear Hear. 24, 332–341.

Avraham, K.B., Hasson, T., Steel, K.P., Kingsley, D.M., Russell, L.B., Mooseker, M.S., Copeland, N.G., Jenkins, N.A., 1995. The mouse Snell's waltzer deafness gene encodes an unconventional myosin required for structural integrity of inner ear hair cells. Nat. Genet. 11, 369–375.

Biemesderfer, D., Mentone, S.A., Mooseker, M., Hasson, T., 2002. Expression of myosin VI within the early endocytic pathway in adult and developing proximal tubules. Am. J. Physiol. Renal. Physiol. 282, F785–F794.

Breckler, J., Au, K., Cheng, J., Hasson, T., Burnside, B., 2000. Novel myosin VI isoform is abundantly expressed in retina. Exp. Eye Res. 70, 121–134.

Buss, F., Kendrick-Jones, J., Lionne, C., Knight, A.E., Cote, G.P., Paul Luzio, J., 1998. The localization of myosin VI at the golgi complex and leading edge of fibroblasts and its phosphorylation and recruitment into membrane ruffles of A431 cells after growth factor stimulation. J. Cell Biol. 143, 1535–1545.

Buss, F., Arden, S.D., Lindsay, M., Luzio, J.P., Kendrick-Jones, J., 2001. Myosin VI isoform localized to clathrin-coated vesicles with a role in clathrin-mediated endocytosis. EMBO J. 20, 3676–3684.

Buss, F., Luzio, J.P., Kendrick-Jones, J., 2002. Myosin VI, an actin motor for membrane traffic and cell migration. Traffic 3, 851–858.

Deng, W., Leaper, K., Bownes, M., 1999. A targeted gene silencing technique shows that *Drosophila* myosin VI is required for egg chamber and imaginal disc morphogenesis. J. Cell Sci. 112, 3677–3690.

Ernest, S., Rauch, G.J., Haffter, P., Geisler, R., Petit, C., Nicolson, T., 2000. Mariner is defective in myosin VIIA: a zebrafish model for human hereditary deafness. Hum. Mol. Genet. 9, 2189–2196.

Force, A., Lynch, M., Pickett, F.B., Amores, A., Yan, Y.L., Postlethwait, J., 1999. Preservation of duplicate genes by complementary, degenerative mutations. Genetics 151, 1531–1545.

Geisbrecht, E.R., Montell, D.J., 2002. Myosin VI is required for E-cadherin-mediated border cell migration. Nat. Cell Biol. 4, 616–620.

Granato, M., van Eeden, F.J., Schach, U., Trowe, T., Brand, M., Furutani-Seiki, M., Haffter, P., Hammerschmidt, M., Heisenberg, C.P., Jiang, Y.J., Kane, D.A., Kelsh, R.N., Mullins, M.C., Odenthal, J., Nusslein-Volhard, C., 1996. Genes controlling and mediating locomotion behavior of the zebrafish embryo and larva. Development 123, 399–413.

Haddon, C., Lewis, J., 1996. Early ear development in the embryo of the zebrafish, *Danio rerio*. J. Comp. Neurol. 365, 113–128.

Haffter, P., Granato, M., Brand, M., Mullins, M.C., Hammerschmidt, M., Kane, D.A., Odenthal, J., van Eeden, F.J., Jiang, Y.J., Heisenberg, C.P., Kelsh, R.N., Furutani-Seiki, M., Vogelsang, E., Beuchle, D., Schach, U., Fabian, C., Nusslein-Volhard, C., 1996. The identification of genes with unique and essential functions in the development of the zebrafish, *Danio rerio*. Development 123, 1–36.

Hammerschmidt, M., Pelegri, F., Mullins, M.C., Kane, D.A., van Eeden, F.J., Granato, M., Brand, M., Furutani-Seiki, M., Haffter, P., Heisenberg, C.P., Jiang, Y.J., Kelsh, R.N., Odenthal, J., Warga, R.M., Nusslein-Volhard, C., 1996. *dino* and *mercedes*, two genes regulating dorsal development in the zebrafish embryo. Development 123, 95–102.

Hasson, T., 2003. Myosin VI: two distinct roles in endocytosis. J. Cell Sci. 116, 3453–3461.

Hasson, T., Mooseker, M.S., 1994. Porcine myosin-VI: characterization of a new mammalian unconventional myosin. J. Cell Biol. 127, 425–440.

Hasson, T., Mooseker, M.S., 1996. Vertebrate unconventional myosins. J. Biol. Chem. 271, 16431–16434.

Hasson, T., Gillespie, P.G., Garcia, J.A., MacDonald, R.B., Zhao, Y., Yee, A.G., Mooseker, M.S., Corey, D.P., 1997. Unconventional myosins in inner-ear sensory epithelia. J. Cell Biol. 137, 1287–1307.

Homma, K., Yoshimura, M., Saito, J., Ikebe, R., Ikebe, M., 2001. The core of the motor domain determines the direction of myosin movement. Nature 412, 831–834.

Kelleher, J.F., Mandell, M.A., Moulder, G., Hill, K.L., L'Hernault, S.W., Barstead, R., Titus, M.A., 2000. Myosin VI is required for asymmetric segregation of cellular components during *C. elegans* spermatogenesis. Curr. Biol. 10, 1489–1496.

Kellerman, K.A., Miller, K.G., 1992. An unconventional myosin heavy chain gene from *Drosophila melanogaster*. J. Cell Biol. 119, 823–834.

Knapik, E.W., Goodman, A., Ekker, M., Chevrette, M., Delgado, J., Neuhauss, S., Shimoda, N., Driever, W., Fishman, M.C., Jacob, H.J., 1998. A microsatellite genetic linkage map for zebrafish (*Danio rerio*). Nat. Genet. 18, 338–343.

Lanford, P.J., Platt, C., Popper, A.N., 2000. Structure and function in the saccule of the goldfish (*Carassius auratus*): a model of diversity in the non-amniote ear. Hear. Res. 143, 1–13.

Melchionda, S., Ahituv, N., Bisceglia, L., Sobe, T., Glaser, F., Rabionet, R., Arbones, M.L., Notarangelo, A., Di Iorio, E., Carella, M., Zelante, L., Estivill, X., Avraham, K.B., Gasparini, P., 2001. *MYO6*, the human homologue of the gene responsible for deafness in Snell's waltzer mice, is mutated in autosomal dominant nonsyndromic hearing loss. Am. J. Hum. Genet. 69, 635–640.

Nicolson, T., Rusch, A., Friedrich, R.W., Granato, M., Ruppersberg, J.P., Nusslein-Volhard, C., 1998. Genetic analysis of vertebrate sensory hair cell mechanosensation: the zebrafish circler mutants. Neuron 20, 271–283.

Nishikawa, S., Homma, K., Komori, Y., Iwaki, M., Wazawa, T., Hikikoshi Iwane, A., Saito, J., Ikebe, R., Katayama, E., Yanagida, T., Ikebe, M., 2002. Class VI myosin moves processively along actin filaments backward with large steps. Biochem. Biophys. Res. Commun. 290, 311–317.

Petritsch, C., Tavosanis, G., Turck, C.W., Jan, L.Y., Jan, Y.N., 2003. The *Drosophila* myosin VI Jaguar is required for basal protein targeting and correct spindle orientation in mitotic neuroblasts. Dev. Cell 4, 273–281.

Prince, V.E., Pickett, F.B., 2002. Splitting pairs: the diverging fates of duplicated genes. Nat. Rev. Genet. 3, 827–837.

Quint, E., Steel, K.P., 2003. Use of mouse genetics for studying inner ear development. Curr. Top. Dev. Biol. 57, 45–83.

Schulte-Merker, S., Hammerschmidt, M., Beuchle, D., Cho, K.W., De Robertis, E.M., Nusslein-Volhard, C., 1994. Expression of zebrafish goosecoid and no tail gene products in wild-type and mutant no tail embryos. Development 120, 843–852.

Seiler, C., Nicolson, T., 1999. Defective calmodulin-dependent rapid apical endocytosis in zebrafish sensory hair cell mutants. J. Neurobiol. 41, 424–434.

Self, T., Sobe, T., Copeland, N.G., Jenkins, N.A., Avraham, K.B., Steel, K.P., 1999. Role of myosin VI in the differentiation of cochlear hair cells. Dev. Biol. 214, 331–341.

Talbot, W.S., Schier, A.F., 1999. Positional cloning of mutated zebrafish genes. Methods Cell Biol. 60, 259–286.

Taylor, J.S., Braasch, I., Frickey, T., Meyer, A., Van de Peer, Y., 2003. Genome duplication, a trait shared by 22 000 species of ray-finned fish. Genome Res. 13, 382–390.

Warner, C.L., Stewart, A., Luzio, J.P., Steel, K.P., Libby, R.T., Kendrick-Jones, J., Buss, F., 2003. Loss of myosin VI reduces secretion and the size of the Golgi in fibroblasts from Snell's waltzer mice. EMBO J. 22, 569–579.

Wells, A.L., Lin, A.W., Chen, L.Q., Safer, D., Cain, S.M., Hasson, T., Carragher, B.O., Milligan, R.A., Sweeney, H.L., 1999. Myosin VI is an actin-based motor that moves backwards. Nature 401, 505–508.

Whitfield, T.T., 2002. Zebrafish as a model for hearing and deafness. J. Neurobiol. 53, 157–171.

Whitfield, T.T., Granato, M., van Eeden, F.J., Schach, U., Brand, M., Furutani-Seiki, M., Haffter, P., Hammerschmidt, M., Heisenberg, C.P., Jiang, Y.J., Kane, D.A., Kelsh, R.N., Mullins, M.C., Odenthal, J., Nusslein-Volhard, C., 1996. Mutations affecting development of the zebrafish inner ear and lateral line. Development 123, 241–254.